doi: 10.12029/gc20210305

刘俊,李文昌,周清,杨富成,姜晓佳,张树志,郭欣然. 2021. 斑岩型钨矿床研究进展[J]. 中国地质, 48(3): 732−748.

Liu Jun, Li Wenchang, Zhou Qing, Yang Fucheng, Jiang Xiaojia, Zhang Shuzhi, Guo Xinran. 2021. Advances in the study of porphyry tungsten deposits[J]. Geology in China, 48(3): 732−748(in Chinese with English abstract).

斑岩型钨矿床研究进展

刘俊[1],李文昌[1,2,3],周清[1],杨富成[3],姜晓佳[2],张树志[4],郭欣然[5]

(1.中国地质调查局成都地质调查中心,四川 成都 610081;2.中国地质大学(武汉)资源学院,湖北 武汉 430074;
3.中国地质大学(北京)地球科学与资源学院,北京 100083;4.桂林理工大学南宁分校,广西 南宁 530001;
5.广东省地质科普教育馆,广东 广州 510000)

提要:斑岩型钨矿床是全球第三重要的钨矿类型,但对其研究较为薄弱、零散。文章基于团队近年来对斑岩钨矿床的研究并系统搜集了全球的相关资料,然后对其进行梳理与总结。研究表明,斑岩型钨矿主要分布于环太平洋成矿带与阿尔卑斯—喜马拉雅成矿带,岩浆弧、板内及陆−陆碰撞等多种环境均有矿床产出。矿床绝大多数形成于中生代、少量形成于古生代。斑岩型钨矿化与弱氧化、较高分异程度的I型或A型花岗质浅成侵入体密切相关。成矿有关岩浆岩主要起源于古老地壳的重熔,并有少量亏损地幔和/或海洋沉积物的混染。成矿流体、金属元素等主要来自于相关的岩浆岩,成矿所需的钙、铁、锰可由地层与岩浆岩通过水岩反应共同提供。岩浆弧及板内环境下初始成矿流体多属于中高温、中高盐度的NaCl−H_2O系统,大陆碰撞体系下则多属于中高温、中低盐度的NaCl−H_2O−CO_2体系。钨在熔−流体分异过程中倾向于富集在共存的流体相,然后以单体钨酸盐、多钨酸盐及氟钨酸盐类等形式迁移。矿质沉淀机制主要包括流体不混溶/沸腾/CO_2逃逸±流体混合和水岩反应。白钨矿和黑钨矿作为斑岩钨矿床中最重要的两种钨矿物,其产出可能主要受控于相关岩浆−流体系统中F含量的高低。

关 键 词:斑岩型钨矿床;时空分布;岩浆系统;成矿作用;地质调查工程

中图分类号:P618.67 **文献标志码**:A **文章编号**:1000−3657(2021)03−0732−17

Advances in the study of porphyry tungsten deposits

LIU Jun[1], LI Wenchang[1,2,3], ZHOU Qing[1], YANG Fucheng[3], JIANG Xiaojia[2],
ZHANG Shuzhi[4], GUO Xinran[5]

(1.*Chengdu Center of China Geological Survey, Chengdu* 610081*, Sichuan, China;* 2.*Faculty of Earth Resources, China University of Geosciences, Wuhan* 430074*, Hubei, China;* 3.*School of Earth Science and Resources, China University of Geosciences, Beijing* 100083*, China;* 4.*Guilin University of Technology at Nanning, Nanning* 530001*, Guangxi, China;* 5.*The Geological Science Education Center of Guangdong Province, Guangzhou* 510000*, Guangdong, China*)

收稿日期:2020−11−17;**改回日期**:2021−04−19

基金项目:国家自然科学基金重大研究计划(92055314)、云南省科学技术奖−杰出贡献奖项目(2017001)与四川省"天府万人计划"杰出科学家项目(川万人第023号)联合资助。

作者简介:刘俊,男,1990年生,博士,助理工程师,从事青藏高原及邻区地质矿产研究;E−mail:cdzxlj2017@163.com。

通讯作者:李文昌,男,1962年生,教授,博士生导师,从事找矿勘查与地质矿产研究;E−mail:Lwcyndd@163.com。

Abstract: P Porphyry tungsten deposit is the third most important type in the world, but its research is weak and scattered. This paper systematically summarizes and analyzes the research results in recent years from our team and other scholars about porphyry tungsten deposits. The results show that porphyry tungsten deposits are widely distributed in the Circum−Pacific metallogenic belt and the Alps−Himalayan metallogenic belt, and occur in magmatic arc, intraplate, and continental collision settings. Most of them were formed in Mesozoic and a few in Paleozoic. Porphyry tungsten mineralization is closely related to weakly oxidized, highly fractionated I− type or A− type hypabyssal granitic rocks, which were mainly derived from re− melting of the ancient crust, contaminated with a small amount of juvenile crust and/ or depleted mantle and/ or marine sediments. The ore−forming metals and fluids were dominantly originated from related magmatic rocks, and the Ca^{2+}, Fe^{2+}, and Mn^{2+} needed for W mineralization could be provided by the strata and magmatic rocks through water− rock reaction. The initial ore− forming fluids of porphyry tungsten deposits in magma arc and intraplate settings belong to the NaCl− H_2O system with medium− high temperature, medium− high salinity and low CO_2 content, while those under continental collision setting belong to NaCl−H_2O−CO_2 system with medium−high temperature, medium−low salinity and high CO_2 content. W tends to be enriched in the coexisting fluid phase in the process of melt−fluid differentiation, and then migrates in the form of monomer tungstate, polytungstate, and fluorotungstate. The mechanisms of mineral precipitation mainly include fluid immiscibility/ boiling/ CO_2 escape ± fluid mixing and water− rock reaction. Scheelite and wolframite are the dominant W−bearing minerals in porphyry tungsten deposits, and their occurrence may be mainly controlled by the fluorine content in relevant magma−fluid system.

Key words: porphyry tungsten deposit; temporal and spatial distributions; magma system; ore− forming processes; geological survey engineering

About the first author: LIU Jun, male, born in 1990, doctor, assistant engineer, engaged in the study of geology and mineral resources in the Tibetan Plateau and its adjacent areas; E−mail: cdzxlj2017@163.com.

About the corresponding author: LI Wenchang, male, born in 1962, professor, doctoral supervisor, engaged in geological prospecting and research; E−mail: Lwcyndd@163.com.

Fund support: Funded by the major research projects of the National Natural Science Foundation of China (No.92055314), the Yunnan Science and Technology Award−Outstanding Contribution Award (No.2017001), and the Outstanding Scientist Award of " Tianfu Ten Thousand People Plan " in Sichuan Province (No. 023).

1 引 言

钨素有“工业牙齿”之称,是重要的战略性矿产资源(李宪海等,2014;Fortier et al., 2018;Calvo et al., 2019)。钨矿床种类众多,主要包括石英脉型、矽卡岩型、云英岩型、斑岩型、蚀变花岗岩型、角砾岩型、陆相火山岩型、层控型、风化壳−砂岩型、现代热泉沉积型、含钨卤水−蒸发岩型和伟晶岩型(徐克勤等,1959;石洪召等,2009;Sheng et al., 2015;蒋少涌等,2020;毛景文等,2020)。世界范围内,矽卡岩型和石英脉型钨矿床占据统治地位(Sheng et al., 2015),从而吸引了众多学者的持续关注(Lu et al., 2003;Selby et al., 2003;丰成友等,2011;袁顺达等,2012;祝新友等,2013;Dewaele et al., 2016; Pan et al., 2018;李佳黛和李晓峰,2020)。斑岩型钨矿床作为世界上储量排在第三位的钨矿床类型(BGS, 2011),但对其研究较为薄弱、零散。20世纪70—90年代,时值全球研究斑岩铜、钼矿的热潮,斑岩钨矿也迎来了一个找矿与研究的“黄金时代”,发现的代表性矿床包括Northern Dancer(Noble et al., 1984)、Mount Pleasant(Davis and Williams− Jones, 1985; Kooiman et al., 1986)、Sisson Brook(Nast and Williams−Jones, 1991)、阳储岭(张玉学,1982;莫名滇,1988)、莲花山(谭运金,1985)等。古菊云(1988)与Sinclair(1995)曾对上述斑岩型钨矿床的成矿地质背景、矿化特征、成矿时代、成矿岩体特征、成矿流体特征等方面进行了概略性的总结,为进一步的找矿与研究工作奠定了良好的基础。然而,20世纪发现的这些矿床规模不是很大、经济价值偏小(Sinclair, 1995),随后的勘查与研究工作便陷入了停滞。最近十多年来随着中国地质调查工程的稳步推进,福建行洛坑(张家菁等,2008)、安徽东源(杜玉雕等,2011)、湖南木瓜园(Li et al., 2018)、西藏拉荣(刘俊等,2019)等一批中—大型斑岩钨矿床相继被发现,

在全球产生了重要的冲击作用(毛景文等,2020)。当前,斑岩钨矿床已经成为了钨矿的重要找矿方向,相关的勘查与研究工作即将掀起一个新的高潮。

随着近些年斑岩钨矿床不断地实现找矿突破并取得研究新进展,相关认识亟待系统总结、梳理与更新。本文基于团队近年来对斑岩型钨矿床的深入研究,并系统搜集了其他相关资料,对斑岩钨矿床的时空分布规律、成矿特征、成矿岩体特征、成矿物质来源、成矿流体特征、钨的分配、迁移及沉淀机制等方面进行系统的总结,以期为未来斑岩钨矿床的研究与找矿勘查工作提供参考。

2　斑岩型钨矿的时空分布规律

全球斑岩钨矿床主要分布于广义上的环太平洋成矿带,其次分布于阿尔卑斯—喜马拉雅成矿带(徐克勤等,1959;BGS, 2011;Sheng et al., 2015;图1)。代表性矿床包括加拿大的Northern Dancer、Mount Pleasant、Sisson Brook,中国的阳储岭、东源、莲花山、木瓜园、行洛坑、拉荣(表1)。不同于斑岩型铜、钼矿床全球的大量分布(分别占据了全球约75%和50%的资源量;Sillitoe, 2010),斑岩型钨矿床的分布较少,资源量占比较低(16%;BGS, 2011)。是由于大量斑岩钨矿床因成矿深度较大(毛景文等,2020)而未被揭露,或是因为钨元素特殊的地球化学性质(Wood and Samson, 2000)更有利于矽卡岩型或石英脉型钨矿床的形成?其内在制约因素尚需要进一步的研究。

全球斑岩型钨矿床产出时间相对较为集中,绝大多数形成于中生代(尤以晚侏罗—早白垩世居多),少量形成于古生代(图2)。同其他类型钨矿床一致,具有中生代大爆发的特点(Sheng et al., 2015)。

3　斑岩型钨矿的成矿地质背景

Sinclair(1995)基于加拿大与中国少量斑岩型钨矿床成矿背景的研究提出其主要形成于克拉通弱—中度伸展带,特别是加厚地区的后碰撞环境。Mao et al.(2013)通过系统梳理华南地区的构造-岩浆-成矿作用,提出造山运动之后的陆内环境对钨矿成矿较为有利。Mao et al.(2017)、Zhao et al.(2017)、Liu et al.(2018)认为华南大量的W-Sn-Cu-Mo矿化与古太平洋板块的俯冲相关。刘俊等(2019)基于区域地质背景分析,提出藏东晚白垩世

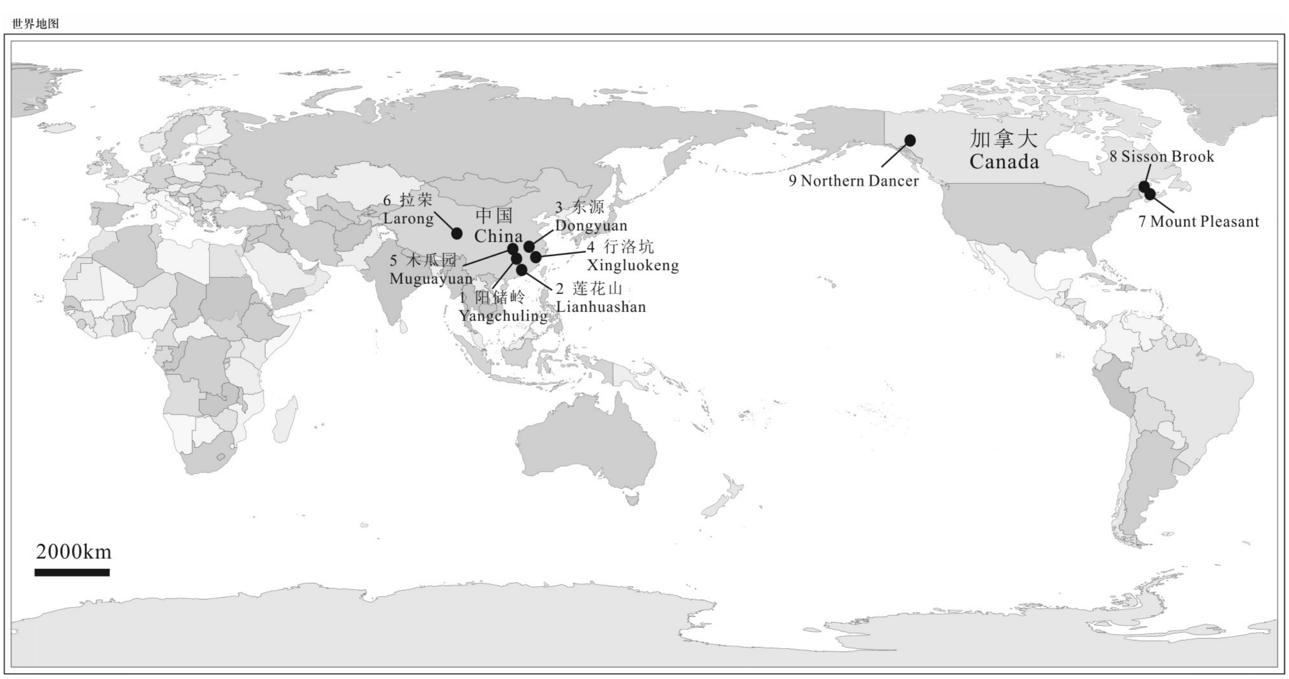

图1　全球斑岩型钨矿床空间分布图
(底图自https://www.vecteezy.com/free-vector/world-map;矿床位置据表1及参考文献)
Fig.1　Distribution of porphyry tungsten deposits in the world
(The background map is after https://www.vecteezy.com /free-vector/world-map, and the location of the deposits is shown in Table 1 and its references)

表1 全球典型斑岩钨矿床一览

Table 1 Characteristics of representative porphyry tungsten deposits in the world

序号	矿床名称	成矿组合	储量及品位	成矿时代/Ma	构造环境	成矿岩体	成矿围岩	矿化特征	矿石矿物	脉石矿物	围岩蚀变	流体特征	成矿机制	物质来源	参考文献
1	阳储岭	W-Mo	WO_3 63100 t，0.2%；Mo 16900t，0.03%～0.06%	146.4± 1.0	古太平洋俯冲体制	I型二长花岗斑岩	新元古界双桥山群千枚岩、板岩及粉砂岩	网脉状、浸染状矿化，具有上钨下钼的特点	白钨矿、辉钼矿、黄铁矿、磁黄铁矿、黄铜矿、闪锌矿、方铅矿、辉铋矿	石英、钾长石、白云母、绢云母、绿泥石、碳酸盐矿物	角岩化、钾化、硅化、钠长石化、碳酸盐化、绢云母化	均一温度160~340℃，盐度11%~55%，可见一定的石盐子矿物，含微量的CO_2	流体沸腾	古老地壳+少量地幔	王莉娟等，2011；Mao et al., 2017a
2	莲花山	W	WO_3 35000 t，0.54%	133.2± 0.9	古太平洋俯冲体制	A/I型石英斑岩	早三叠世小坪组砂岩	浸染状、网脉状、脉状	黑钨矿、白钨矿、黄铁矿、磁黄铁矿、毒砂、黄铜矿、方铅矿、锡石	石英、钾长石、黑云母、白云母、绢云母、电气石、方解石、绿泥石	钾化（黑云母化）、云英岩化、绿泥石化、绢云母化、碳酸盐化	均一温度210~420℃，盐度2%~33%，可见一定的石盐子矿物，含微量的CO_2	流体沸腾和流体混合	古老地壳+少量地幔	Lu, 1985；谭运金，1985；Liu et al., 2018
3	东源	W-Mo	WO_3 14000 t	146.4± 2.3	古太平洋俯冲体制	I型花岗闪长斑岩	中元古界牛屋组板岩、千枚岩、粉砂岩	细脉浸染状、浸染状矿化，具上钨下钼的特点	辉钼矿、黄铁矿、白钨矿、赤铁矿	石英、钾长石、斜长石、黑云母、绢云母、绿泥石、方解石、萤石	角岩化、硅化、钾化、绢云母化、绿泥石化、绿帘石化和碳酸盐化	均一温度138~354℃，盐度1%~9%，可见一定的CO_2型包裹体	水岩反应	古老地壳+少量地幔	秦燕等，2010；杜玉雕等，2011；Wang et al., 2017
4	行洛坑	W-Mo	WO_3 304300 t，0.23%	156.3 ± 4.8	古太平洋俯冲体制	斑状黑云母花岗岩	震旦系罗峰溪群（粉）砂岩	浸染状、脉状矿化，矿化集中于矿体上部	黑钨矿、白钨矿、辉钼矿、锡石、闪锌矿、黄铜矿	石英、黑云母、钾长石、萤石、方解石、绿泥石、高岭石	钾长石化、云英岩化、绢英岩化、钠长石化、绿泥石化、硅化	-	-	-	张家菁等，2008；Zhao et al., 2017
5	木瓜园	W-Mo	WO_3 5300 t，0.12%	225.4 ± 1.4	后碰撞	花岗斑岩	新元古界马底驿组粉砂质板岩、砂岩	浸染状、细脉状和网脉状	白钨矿，黄铁矿、辉钼矿、毒砂	长石、石英、绢云母、高岭土、绿泥石、方解石	绢云母化、硅化、云英岩化、绿泥石化	-	水岩反应	古老地壳	Li et al., 2018；李洪英等，2019；陕亮等，2019

续表1

序号	矿床名称	成矿组合	储量及品位	成矿时代/Ma	构造环境	成矿岩体	成矿围岩	矿化特征	矿石矿物	脉石矿物	围岩蚀变	流体特征	成矿机制	物质来源	参考文献
6	拉荣	W-Mo	WO_3 114800 t，0.1723%；Mo 26000 t，0.0772%	91.8±0.5	后碰撞	I型二长花岗斑岩	西西群石英片岩、绿片岩、三叠纪—白垩纪花岗(斑)岩	浸染状、细脉状和网脉状	白钨矿、辉钼矿、黄铁矿、黄铜矿、金红石、斜方辉铋铅矿、锡石及毒砂	石英、长石、绢云母、白云母、绿泥石、方解石、绿帘石、萤石	角岩化、绢英岩化、云英岩化、钾化、绿泥石化、高岭土化、碳酸盐化、叶蜡石化、萤石化	均一温度270~440℃，盐度2%~14%，可见大量CO_2型包裹体	水岩反应	古老地壳+少量地幔	刘俊等，2019；Liu et al., 2020a, b, c
7	Mount Pleasant	W-Mo	45 Mt矿石：WO_3，0.2%，Mo，0.1%	370±2	板内环境	A型石英二长斑岩	志留—泥盆纪黏土岩、杂砂岩	浸染状、脉状、豆荚状矿化	黑钨矿、白钨矿、闪锌矿、毒砂、天然铋、黄铜矿、方铅矿、锡石	石英、萤石、黄玉、绿泥石、黑云母、钾长石、绢云母、方解石	云英岩化、绢英岩化、绿泥石化、黄玉化、高岭土化、钾化	均一温度260~490℃，盐度10%~42%，可见一定的石盐子矿物，含微量的CO_2	流体沸腾	-	Davis and Williams-Jones, 1985；Inverno and Hutchinson, 2006；Thorne et al., 2013
8	Sisson Brook	W-Mo-Cu	387 Mt矿石：WO_3，0.067%，Mo，0.021%	419～422	后碰撞	黑云母花岗岩/石英斑岩	板岩、石英岩、长英质变火山岩	网脉状、细脉状矿化	黑钨矿、白钨矿、辉钼矿、黄铜矿、磁黄铁矿、闪锌矿、方铅矿、自然铋	石英、角闪石、钠长石、钾长石、黑云母、萤石、方解石	角闪石化、钠化、磁铁矿化、钾化、黑云母化、绿泥石化、碳酸盐化、萤石化	均一温度330~430℃，可见一定的石盐子矿物	水岩反应	-	Nast and Williams-Jones., 1991；Zhang et al., 2016, 2020
9	Northern Dancer	W-Cu-Mo	162 Mt矿石：WO_3，0.13%，Mo，0.052%	108	板内环境	A/I型斑状二长花岗岩	黑云母石英岩、角页岩、矽卡岩	网脉状、细脉状矿化	白钨矿、辉钼矿、黄铁矿、磁黄铁矿、黄铜矿、闪锌矿、自然铋	绿帘石、长石、黑云母、萤石、石榴子石、透辉石、方解石、绿泥石、绢云母	绢云母化、碳酸盐化、萤石化、绿帘石化、绿泥石化	均一温度240~430℃，盐度3%~39%，可见一定石盐子矿物	水岩反应	-	Noble et al., 1984；Mortensen et al., 2006；Brand, 2008

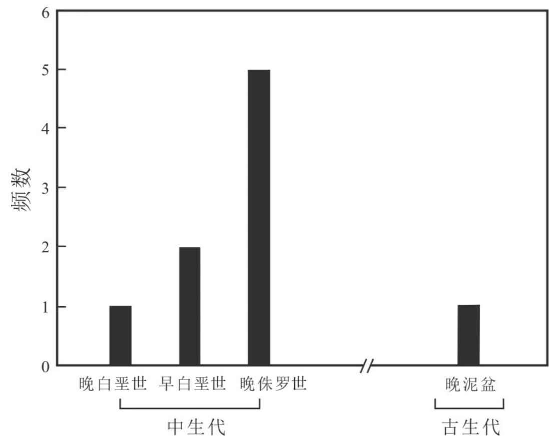

图2 全球斑岩型钨矿床时间分布图
(据 Mortensen et al., 2006;张家菁等,2008;周翔等,2011;Thorne et al., 2013;Mao et al., 2017a;Liu et al., 2018;李洪英等,2019;刘俊等,2019;Zhang et al., 2020)
Fig.2 Histogram showing the ore-forming ages of porphyry tungsten deposits in the world
(after Mortensen et al., 2006; Zhang Jiajing et al., 2008; Zhou Xiang et al., 2011; Thorne et al., 2013; Mao et al., 2017a; Liu et al., 2018; Li Hongying et al., 2019; Liu Jun et al., 2019; Zhang et al.,2020)

拉荣斑岩钨钼矿床形成于碰撞造山环境。王登红等(2014)认为古老结合带及其早期发育的古深大断裂对钨矿床形成具有明显的制约作用,该观点也得到了其他学者的支持(如刘俊等,2019)。由此可见,如同斑岩型铜矿床一样(Sillitoe, 2010;Cooke et al., 2014;侯增谦等,2020),斑岩型钨矿床可以形成于岩浆弧、板内及陆-陆碰撞等多种环境,早期发育的区域性构造对于矿床的分布起到明显的制约作用。

4 斑岩型钨矿的成矿地质特征

斑岩型钨矿床成矿围岩地层主要为一套浅变质岩、碎屑岩及少量的页岩、火成岩等(表1)。例如,阳储岭矿床的赋矿围岩为一套千枚岩、板岩及粉砂岩(Mao et al., 2017);拉荣矿床的赋矿围岩为一套石英片岩、绿片岩及花岗(斑)岩体(刘俊等,2019);Sisson Brook矿床的赋矿围岩为一套板岩、石英岩、长英质变火山岩(Nast and Williams-Jones., 1991)。成矿岩体主要为二长花岗斑岩(阳储岭、拉荣矿床;Mao et al., 2017a;刘俊等,2019)、石英斑岩(Sisson Brook、莲花山矿床;Nast and Williams-Jones., 1991;Liu et al., 2018)、花岗斑岩(木瓜园矿床;李洪英等,2019)、花岗闪长斑岩(东源矿床;秦燕等,2010)、斑状花岗岩(行洛坑矿床;张家菁等,2008)、斑状二长花岗岩(Northern Dancer矿床;Mortensen et al., 2006)、石英二长斑岩(Mount Pleasant矿床;Thorne et al., 2013)等酸性浅成岩浆岩。然而,这些成矿斑岩基本呈似斑状结构,可能反映了斑岩钨矿成矿有关的岩体侵位普遍偏深(毛景文等,2020)。矿床主要位于深大断裂带附近次级断裂交汇处或者转弯处(如拉荣矿床;刘俊等,2019)。斑岩钨矿的围岩蚀变以强云英岩化、弱钾化和弱青磐岩化为特征(Davis and William-Jones, 1985)。类似于斑岩铜矿床(Lowell and Guilbert, 1970;Sillitoe, 2010;Cooke et al., 2014;侯增谦等,2020),一般从斑岩体中心向外依次发育有钾硅化,石英白(绢)云母化,到绿泥石碳酸盐化等蚀变分带(Davis and William- Jones, 1985;莫名浈,1988;Sinclair, 1995)。矿化与蚀变的大致对应关系由内向外依次为W(Mo)带,Mo(W)和黄铁矿化带,并且矿体主要产在石英白(绢)云母化带内(如阳储岭、东源、拉荣;莫名浈,1988;杜玉雕等,2011;刘俊等,2019)。矿体形态多样,呈层状、似层状、囊状、团块状,分布在岩体中上部及内外接触带附近(张玉学,1982;古菊云,1988),个别矿床(如阳储岭;Mao et al., 2017a)顶部可见角砾岩筒。矿石呈浸染状、细脉浸染状产出,且多具有上钨下钼的特点(如阳储岭、东源;莫名浈,1988;杜玉雕等,2011)。金属矿物主要为白钨矿、黑钨矿、辉钼矿、黄铁矿、黄铜矿、锡石、毒砂等,脉石矿物主要为石英、钾长石、白云母、绢云母、黑云母、绿泥石、方解石、萤石等(表1)。

5 斑岩型钨矿的成矿岩浆岩体系

古菊云(1988)指出与斑岩钨矿有关的岩体规模一般小于10 km²,属浅成—超浅成岩株、岩枝和岩墙,在剥蚀程度比较浅的地区,往往与同源火山岩共生。钨元素在地壳中的背景值极低(~1×10^{-6};Rudnick and Gao, 2003),要想富集成矿,其元素含量需要提升n个数量级以上(Lehmann et al., 1990)。因此,斑岩钨矿床的形成一般与长时间、多期次的大规模岩浆作用有关,且成矿多发生在晚期岩浆侵位阶段(Inverno and Hutchinson, 2006;Mao et al., 2017a;Liu et al., 2020b)。斑岩钨矿化与准铝质—弱过铝质、高钾钙碱性—钾玄岩性、中等—高

分异程度的I/A型花岗岩类密切相关（图3a～e；Inverno and Hutchinson, 2006；Mortensen et al., 2006；秦燕等，2010；Mao et al., 2017a；Liu et al., 2018, 2020b），而中国多数石英脉型、矽卡岩型钨矿与S型花岗岩类密切相关（李佳黛和李晓峰，2020；蒋少涌等，2020）。斑岩钨矿成矿有关岩浆岩多属于相对富F的花岗岩（Noble et al., 1984；Davis and William- Jones, 1985；Nast and William- Jones, 1991；张家菁等，2008；杜玉雕等，2011；Mao et al., 2017a；Liu et al., 2020b；Zhang et al., 2020）。研究表明，F的存在有利于增强W、Mo和H_2O等在硅酸盐熔体中的溶解度并且降低岩浆固相线的温度，从而提高岩浆演化的程度和在熔体中W的富集程度，并延缓了含W热液从岩浆中的分离，对于钨的富集具有积极意义（Mustard et al., 2006）。关于岩浆氧逸度与钨矿化的关系，以往多认为还原环境对钨矿床的形成较有利（如Candela, 1992；Mao et al., 2017a），但目前越来越多的证据表明钨矿床与氧逸度的关系并不是十分密切（Blevin, 2004；Wade et al., 2013；Pan et al., 2018），它主要影响Cu、Mo、Sn等伴生元素的富集与否（Shimazaki, 1980；Kwark et al., 1982；Liu et al., 2020b）。前人研究认为Zr/Hf与Nb/Ta比值可用来指示岩浆体系演化程度、岩浆-流体交代作用以及花岗质岩石成矿潜力（Bau et al., 1996；Ballouard et al., 2016；Wu et al., 2017）。斑岩钨矿床成矿岩体的Zr/Hf比值介于7.5～41.4，Nb/Ta比值介于4.1～12.0，基本落在了高分异花岗岩的范围中（Zr/Hf＜38，Nb/Ta＜17；Wu et al., 2017），这与斑岩型钨矿成矿岩石具有较高的岩浆分异指数（*DI*=76～96）相吻合。然而，与Sn-W（U）系列及Ta-Cs-Li-Nb-Be-Sn-W系列成矿有关花岗岩相比（Ballouard et al., 2016），斑岩钨矿床成矿有关岩浆岩的Zr/Hf比值及Nb/Ta比值相对较高（图3f），可能反映了前两者的演化程度或岩浆-热液作用程度更高。斑岩钨矿床成矿有关的岩浆岩在稀土配分模式图上显示出轻稀土富集、重稀土相对亏损，中等—弱负Eu异常的右倾型特征（图4b），而华南钨锡矿床成矿有关岩浆岩具有"海鸥式"稀土元素配分型式和显著的Eu负异常（图4b；Chen et al., 2014；Guo et al., 2015），同样支持上述论断。

斑岩钨矿成矿有关岩浆岩富集大离子亲石元素（Rb、K、Th、U、Pb），亏损高场强元素（Nb、Ta、P、Ti）和Ba、Sr等（图4a），这与成熟的大陆地壳组成十分相似（Rudnick and Gao, 2003），反映了其源区可能主要为壳源物质。成矿有关岩浆岩的$\varepsilon_{Hf}(t)$值变化于-13.0～2.3（图5a），对应的地壳模式年龄变化于1011～2009 Ma（图5c），指示成矿岩浆主要来自于古老地壳的重熔，并有少量亏损地幔物质的混染（周洁，2013；Mao et al., 2017a；Liu et al., 2018, 2020b）。另外，大陆碰撞体系下斑岩钨矿（如拉荣矿床；Liu et al., 2020b）成矿有关岩浆岩呈现出较明显的Nd-Hf同位素解耦（图5b）。前人研究发现"锆石效应"（Carpentier et al., 2009；Tang et al., 2014；Zhang et al., 2019）和"石榴石效应"（Patchett et al., 1984；Schmitz et al., 2004）通常会造成样品出现低$\varepsilon_{Hf}(t)$值的Nd-Hf同位素解耦；而较高$\varepsilon_{Hf}(t)$值的Nd-Hf同位素解耦现象则可能反映了源区有亏损地幔组分（Vervoort and Blichert-Toft, 1999；Sanfilippo et al., 2019）和/或海洋沉积物（Chauvel et al., 2008）的参与。不难理解，在俯冲-碰撞过程中，受沉积物改造的地幔源区可能与重熔的壳源岩浆发生了不同程度的混合（Chauvel et al., 2008；王雪等，2015），从而造成了大陆碰撞体系下斑岩钨矿床成矿有关岩浆岩多呈现高$\varepsilon_{Hf}(t)$值的Nd-Hf同位素解耦。

6 斑岩型钨矿的成矿作用

6.1 成矿物质来源

斑岩型钨矿床是花岗岩岩浆-流体成矿体系的重要组成部分，因此斑岩钨矿床成矿物质来源与岩浆作用密不可分（何兴华和顾尚义，2017；蒋少涌等，2020）。例如，斑岩钨矿床硫化物硫同位素具有明显的塔式正态分布特征，集中于2‰～3‰（图6a），明显不同于沉积岩的S同位素范围（图6b；Seal, 2006），而与磁铁矿-钛铁矿过渡类型花岗岩的范围较为一致。早期研究多认为，钨作为亲石元素，可由（古老）地壳的不断重熔与结晶分异提供（徐克勤，1959；Lehmann et al, 1990；翟裕生，2002；Guo et al., 2015）。在Pb同位素图解（图7a）和$\Delta\beta$-$\Delta\gamma$图解（图7b）上，大多数样品点位于上地壳范围内，少部分落入造山带

和下地壳，也与传统的认识基本一致。然而，与斑岩钨矿床具有成因联系的岩浆岩均为I/A型花

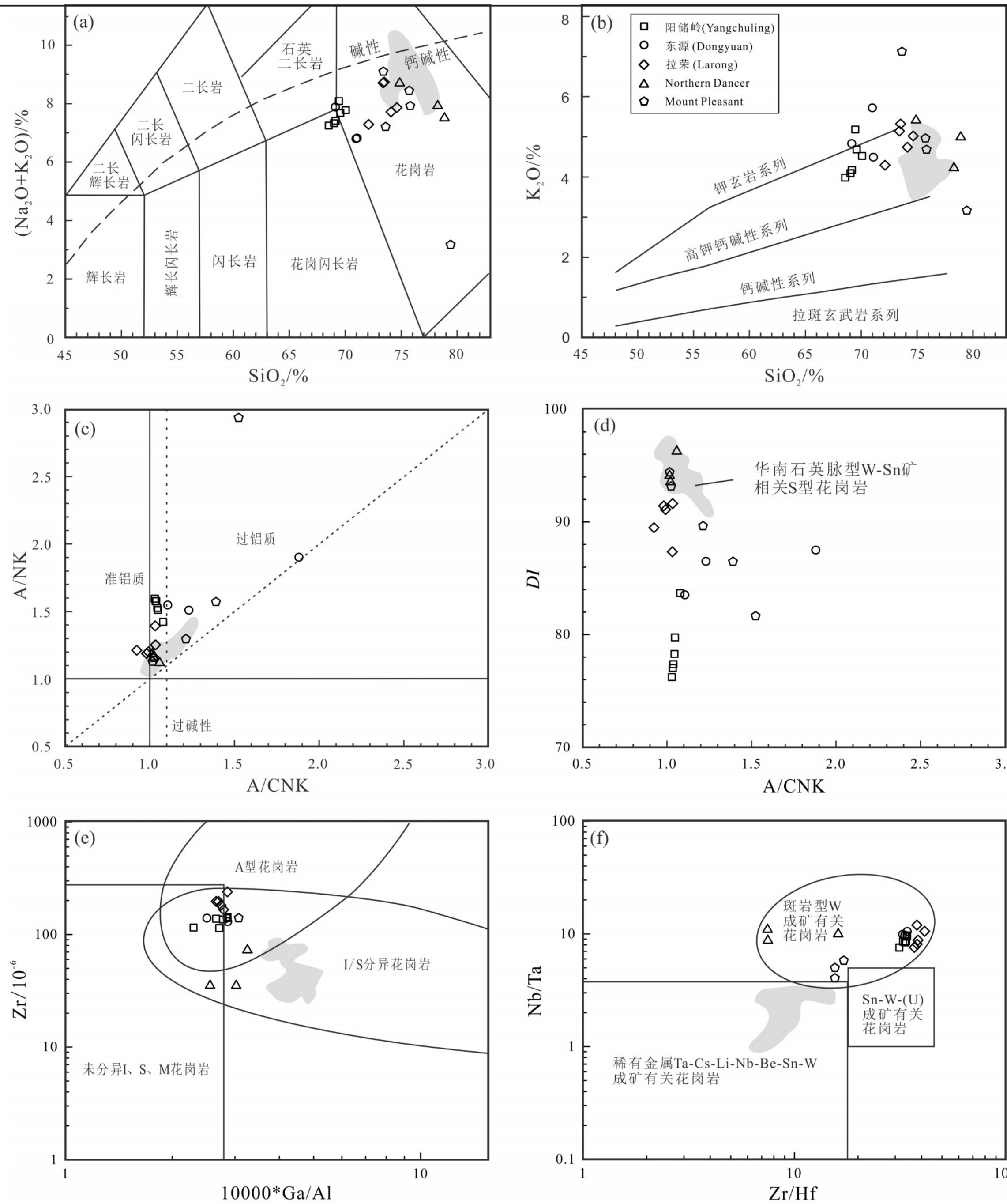

图3 SiO_2−(K_2O + Na_2O)图解(a), SiO_2−K_2O图解(b), A/CNK−A/NK图解(c), A/CNK−DI图解(d), 10000*Ga/Al− Zr图解(e)(据Wu et al., 2017)及Zr/Hf−Nb/Ta 图解(f)(据Ballouard et al., 2016)

(数据引自Inverno and Hutchinson, 2006; Brand, 2008; 周洁, 2013; Chen et al., 2014; Guo et al., 2015; Mao et al., 2017a; Liu et al., 2020b)

Fig.3 (K_2O + Na_2O) vs. SiO_2 diagram (a), K_2O vs. SiO_2 diagram (b), A/NK vs. A/CNK diagram(c), DI vs. A/CNK diagram(d), Zr vs. 10000*Ga/Al diagram(e) (after Wu et al., 2017) and Nb/Ta vs. Zr/Hf diagram (f) (after Ballouard et al., 2016)

(Data sources: Inverno and Hutchinson, 2006; Brand, 2008; Zhou Jie, 2013; Chen et al., 2014; Guo et al., 2015; Mao et al., 2017a; Liu et al., 2020b)

岗岩类(Inverno and Hutchinson, 2006;Mortensen et al., 2006;秦燕等,2010;Mao et al., 2017a;Liu et al., 2018, 2020b),而非陆壳重熔型(即S型)花岗岩,暗示了成矿物质来源的多样性和复杂性(蒋少涌等, 2020)。近年来,精细的Sr−Nd−Hf同位素分析揭示了斑岩钨矿床成矿有关岩浆岩主要起源于古老地壳的重熔,并有少量亏损地幔和/或海洋沉积物的混染(周洁,2013;Mao et al., 2017a;Liu et al., 2018,

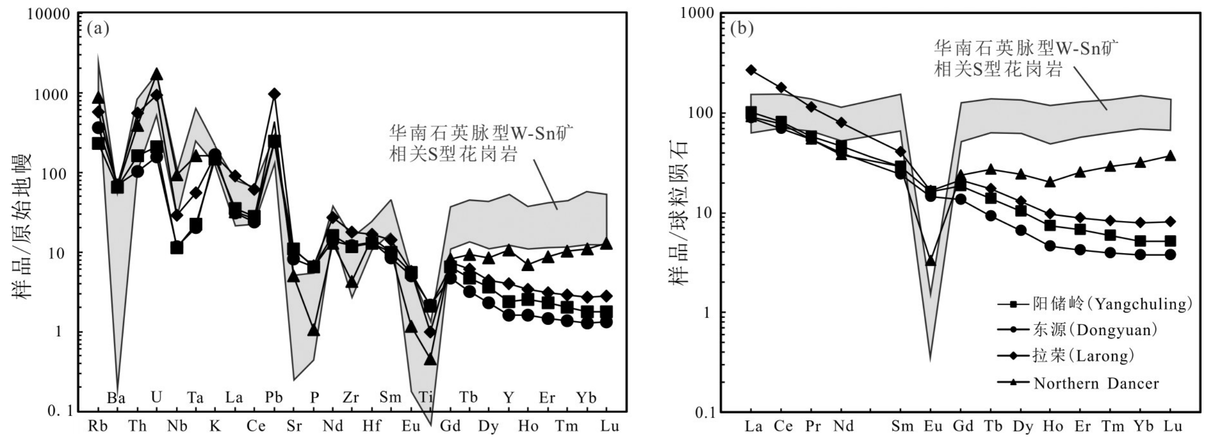

图4 斑岩钨矿床成矿岩体微量元素原始地幔标准化图解(a)和稀土元素球粒陨石标准化图解(b)
(每个矿床采用原始数据的平均值,数据引自Brand, 2008; 周洁, 2013; Chen et al., 2014; Guo et al., 2015; Mao et al., 2017a; Liu et al., 2020b;标准化值据Sun and McDonough,1989)
Fig. 4 Primitive mantle−normalized trace element patterns (a) and chondrite−normalized REE patterns (b) of the ore−related intrusives of porphyry tungsten deposits
(The original data for the average values of each deposits are from Brand, 2008; Zhou Jie, 2013; Chen et al., 2014; Guo et al., 2015; Mao et al., 2017a; Liu et al., 2020b; and values for the chondrite and primitive mantle are from Sun and McDonough ,1989)

2020b);部分学者基于He−Ar、Sr−Nd同位素对钨矿物的直接分析,提出了地幔源区极有可能直接为钨矿化提供了成矿物质(Voicu et al., 2000; Burnard and Polya, 2004)。上述研究指示了壳幔相互作用在斑岩钨矿床成岩成矿过程中扮演着重要的角色(蒋少涌等,2020)。另外,有学者认为围岩可以为矿化提供可观的成矿物质(聂荣锋和王旭东,2007;石洪召等,2009;Liu et al., 2018),具体情况尚需要进一步的研究。

此外,白钨矿/黑钨矿的沉淀不仅需要大量的W、Mo等金属元素,也需要热液中具有足够浓度的阳离子Ca^{2+}、Fe^{2+}、Mn^{2+}等。对于矽卡岩型钨矿床而言,其成矿所需的Ca^{2+}一般来自于富钙灰岩、白云岩等(Pan et al., 2018;李佳黛和李晓峰,2020)。对于缺乏富钙围岩的钨矿床而言,其所需钙元素可从成矿流体中获得(Shabeer et al., 2003),但更主要是通过水岩反应(Nast and Williams− Jones, 1991; Lecumberri−Sanchez et al., 2017; Wang et al., 2017; Zhang et al., 2018; Liu et al., 2020a)提供。例如,周洁(2013)对江南造山带东段东源含矿岩体与非含矿的旌德岩体、桃岭岩体的对比研究发现,含钨花岗岩中斜长石为贫钙的钠长石,因此强烈的水岩反应可能为东源矿床钨的矿化提供了丰富的钙源(Wang et al., 2017);Liu et al.(2020a)对拉荣矿床开展精细解剖,提出花岗闪长斑岩、黑云母花岗斑岩、二长花岗斑岩及围岩绿片岩通过水岩反应共同为白钨矿的沉淀提供了丰富的钙源。

6.2 成矿流体特征及起源

H−O同位素是示踪成矿流体起源及演化的一个有力工具(Taylor, 1974; Meinert, 2003)。笔者系统搜集了全球典型斑岩钨矿床硫化物的H−O同位素数据,发现斑岩钨矿床 $\delta^{18}O_{H_2O}$ 和 δD_{H_2O} 值分别变化于−111.4‰~−54.0‰和−2.6‰~6.9‰(张大椿等,1984; 杜玉雕等,2012; Liu et al., 2020a)。在 $\delta^{18}O_{H_2O}-\delta D_{H_2O}$ 图解中(图8),样品投点均落入岩浆水区域附近,但略低于典型岩浆水(Taylor, 1974)。流体系统亏损 δD_{H_2O} 在世界上其他斑岩矿床中也有广泛记录,可解释为古大气降水与原生成矿流体发生混合(Selby et al., 2001; Wang et al., 2018)或母岩浆的持续脱气作用(Hedenquist et al., 1998; Chelle−Michou et al., 2017)。$\delta^{18}O_{H_2O}$ 值也表现为弱亏损,这通常与水岩反应有关(Harris and Golding, 2002; Wang et al., 2014, 2018; Liu et al., 2020a)。总之,H−O同位素指示斑岩钨矿床初始成矿流体来自于相关岩浆作用,后期可能受大气降水混入±岩浆脱气±水岩反应导致H−O同位素值发生系统降低。

不同构造背景下斑岩钨矿床的成矿流体系统存在较为明显的差异:大多数岩浆弧及板内环境下

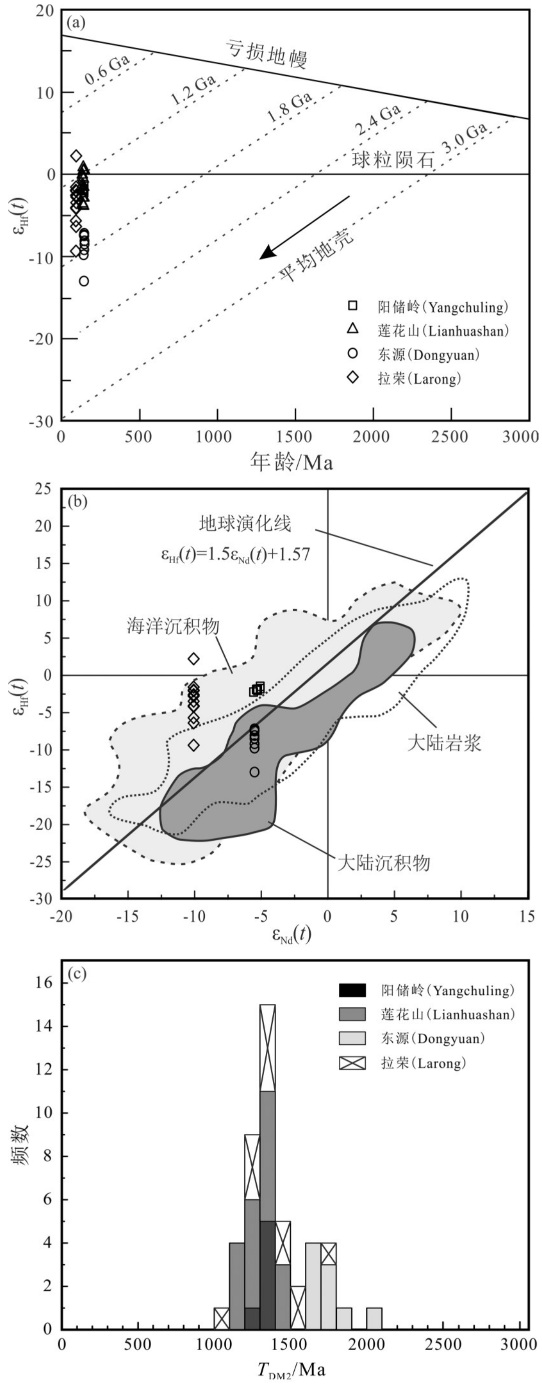

图5 斑岩型钨矿床成矿岩石年龄−$\varepsilon_{Hf}(t)$图解(a),$\varepsilon_{Nd}(t)$−$\varepsilon_{Hf}(t)$图解(b)(底图据 Vervoort et al., 2011; 王雪等,2015)及地壳模式年龄 T_{DM2}分布图(c)

(数据来源:周洁, 2013; Mao et al., 2017a; Liu et al., 2018, 2020b)

Fig.5 Plots of the $\varepsilon_{Hf}(t)$ vs. Ages(a), the $\varepsilon_{Hf}(t)$ vs. $\varepsilon_{Nd}(t)$ (b) (modified from Vervoort et al., 2011; Wang Xue et al., 2015) and the histogram of the two−stage Hf model ages for the ore−related intrusions of porphyry W deposit(c)

(Data sources: Zhou Jie, 2013; Mao et al., 2017a; Liu et al., 2018, 2020b)

斑岩钨矿床(如阳储岭、莲花山、Mount Pleasant、Northern Dancer、Sisson Brook)的成矿流体属于中高温、中高盐度、贫CO_2的NaCl−H_2O系统(包裹体均一温度介于160~490℃,盐度变化于2%~55%,包裹体中可见一定的石盐子矿物,激光拉曼成分分析显示成矿流体中含微量的CO_2(Noble et al., 1984; Lu, 1985; Davis and William−Jones, 1985; Nast and Williams−Jones, 1991; 王莉娟等,2011);而大陆碰撞体系下的斑岩钨矿床(如拉荣)初始成矿流体属于中高温、中低盐度的NaCl−H_2O−CO_2体系(包裹体均一温度介于270~440℃,盐度变化于2%~14%,大量发育富CO_2三相包裹体及一定的纯CO_2相包裹体;Liu et al., 2020a)。关于二者的差异,一个合理的解释是岛弧与板内体系下岩浆的起源有大量洋壳的变质脱水参与,洋壳富H_2O及NaCl,所派生的流体属于中高温、中高盐度的NaCl−H_2O体系,相对贫CO_2;大陆碰撞体系下岩浆的起源有大量大陆地壳的变质脱水参与,陆壳贫H_2O而富钾、CO_2/碳酸盐,所以派生的流体则属于中高温、中低盐度的NaCl−H_2O−CO_2体系,相对富集CO_2(陈衍景和李诺,2009);另一个可能的解释是岛弧与板内体系下斑岩钨矿床成矿流体多发生了流体沸腾使CO_2发生了大量逃逸,而大陆碰撞体系下由于成矿深度偏深(Mao et al., 2017b),成矿流体缺少明显的流体沸腾作用(李佳黛和李晓峰,2020)。

6.3 钨的分配、迁移及沉淀

在自然体系中,钨具有较高的流体亲和性,这会导致在熔−流体分异过程中钨倾向于富集在共存的流体相(Hulsbosch, 2019)。成矿一般始于岩浆演化晚期经液态分异形成的浆液过渡态,之后逐渐演化至岩浆期后热液阶段(祝新友等,2013)。

实验表明,在中性—弱酸性的成矿环境中,钨在高温下(>300℃)主要以单体钨酸盐,如WO_4^{2-}或HWO_4^-等(Keppler and Wyllie, 1991; Wood and Samson, 2000)的形式迁移,相对低温下(<300℃)以多钨酸盐类的形式迁移(Wang et al., 2020),流体盐度可能对钨运移的影响不大(Keppler and Wyllie, 1991)。关于氟在成矿作用中扮演的角色,早期研究认为其存在与钨的迁移没有太大关系,但它可以降低花岗质岩浆的黏度与固相线温度,从而有利于钨在含矿溶液中发生持续的富集(Audétat et al.,

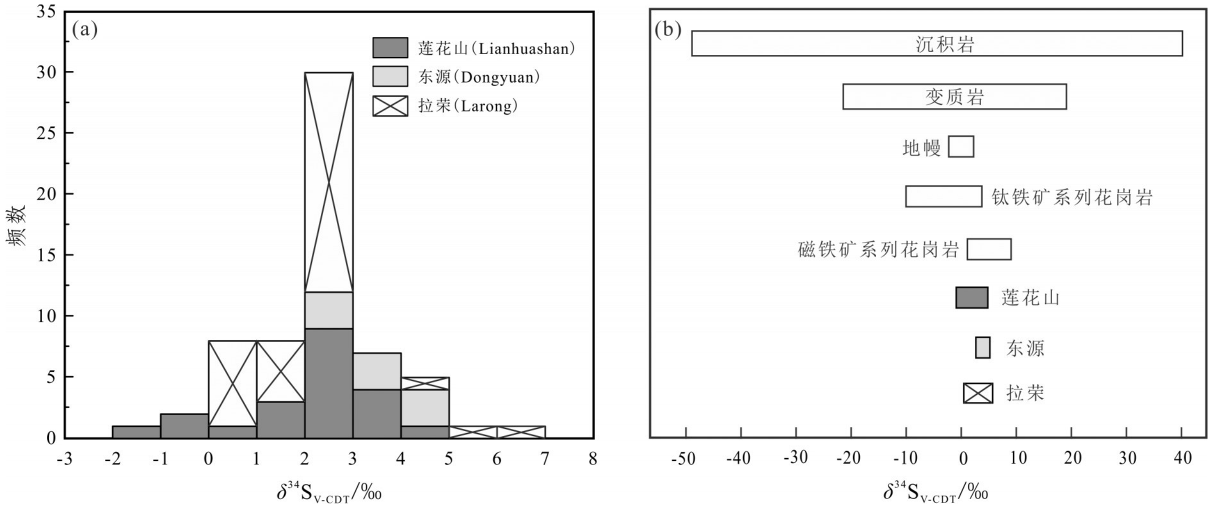

图6 斑岩钨矿床金属硫化物$\delta^{34}S_{VCDT}$值频率直方图及范围图
(数据来源:张理刚, 1985; 杜玉雕等, 2011; Liu et al., 2020c)
Fig.6 Frequency histogram (a) and range (b) of $\delta^{34}S_{VCDT}$ values for metal sulfides from porphyry tungsten deposits
(Data sources: Zhang Ligang, 1985; Du Yudiao et al., 2011; Liu et al., 2020c)

2000);而最近Wang et al.(2021)通过实验模拟研究揭示了在高温酸性(pH < 5)富氟体系中,钨主要以$H_3WO_4F_2^-$的形式运移,且富氟体系比贫氟体系富集钨的能力高10倍左右,则充分说明了氟对于钨的迁移沉淀过程具有积极的作用。关于CO_2是否对钨矿成矿起重要作用,尚存在较大的争议:(1)有学者认为CO_2在成矿中的作用不大或没有起到关键作用(Vallance et al., 2001;Ni et al., 2015);(2)有学者认为CO_2对钨呈WO_4^{2-}形式可能有一定的稳定或保护作用,在成矿中起到了一定的积极作用(许泰等,2012);(3)有学者提出CO_2的逃逸可以调节流体的酸碱度等,在成矿中扮演着极为重要的角色(Wang et al., 2018, 2020)。

研究表明,斑岩钨矿床矿质沉淀机制主要包括以下两种:(1)水岩反应。该机制常常导致温度的降低及斜长石蚀变分解释放Ca^{2+}进入流体等,在斑岩钨矿床矿质沉淀过程中扮演着重要的角色(Nast and Williams−Jones, 1991;Brand, 2008;杜玉雕等,2011;Wang et al., 2017;Li et al., 2018;Liu et al., 2020a);(2)流体不混溶/沸腾/CO_2逃逸±流体混合。

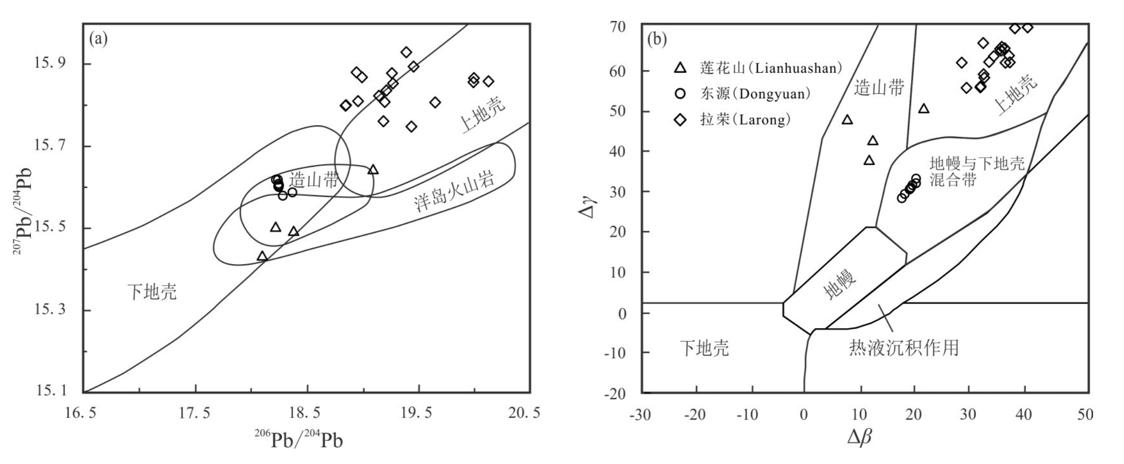

图7 斑岩钨矿床硫化物$^{206}Pb/^{204}Pb-^{207}Pb/^{204}Pb$图解(a, Zartman and Doe, 1981)和$\Delta\beta=-\Delta\gamma$图解(b, 底图据朱炳泉,1998)
(数据来源同图6)
Fig.7 Plot of $^{207}Pb/^{204}Pb$ vs. $^{206}Pb/^{204}Pb$ (a, modified from Zartman and Doe, 1981) and $\Delta\beta$ vs. $\Delta\gamma$ diagram (b, modified from Zhu Bingquan, 1998) of metal sulfides from porphyry tungsten deposits
(Data sources are the same as in Fig. 6)

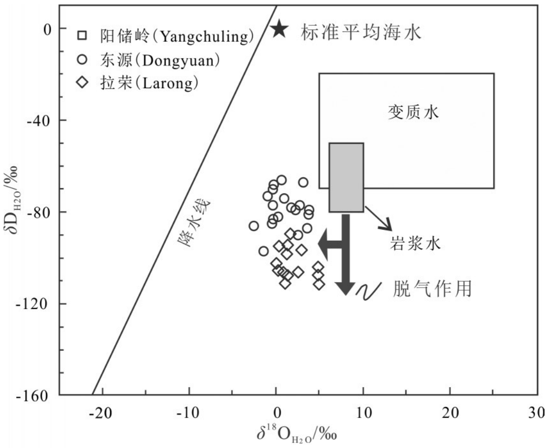

图8 斑岩钨矿床$\delta^{18}O_{H_2O}-\delta D_{H_2O}$关系图(据Taylor, 1974)
(数据来源:张大椿等, 1984; 杜玉雕等, 2011; Liu et al., 2020a)
Fig.8 $\delta^{18}O_{H_2O}$ vs. δD_{H_2O} diagram of porphyry tungsten deposits (after Taylor, 1974).
(Data sources: Zhang Dachun et al., 1984; Du Yudiao et al, 2011; Liu et al., 2020a)

成矿过程中往往伴随着CO_2的不断逃逸,流体的氧逸度不断降低、pH值与S^{2-}逸度不断提高,从而造成了白钨矿、黑钨矿、辉钼矿的相继沉淀(Davis and William−Jones, 1985;Lu, 1985;王莉娟等,2011)。

此外,白钨矿和黑钨矿作为斑岩钨矿床中最重要的两种钨矿物,部分斑岩钨矿床中仅发育白钨矿(如东源、阳储岭、木瓜园、Northern Dancer、拉荣;Noble et al., 1984;杜玉雕等,2011;Mao et al., 2017a;李洪英等,2019;刘俊等,2019),部分斑岩钨矿床中黑钨矿与白钨矿均发育,如莲花山、行洛坑、Mount Pleasant、Sisson Brook(Davis and William−Jones, 1985;Nast and Williams−Jones., 1991;张家菁等,2008;Liu et al., 2018)。是什么因素控制了斑岩钨矿床中钨矿物的种类?徐克勤等(1959)与Lecumberri−Sanchez等(2017)认为钨矿床中白钨矿或者黑钨矿的形成主要取决于Ca^{2+}、Fe^{2+}、Mn^{2+}等元素的丰度,因此围岩岩性在其中起主导作用。谭运金(1999)认为成矿母岩及其演化出的流体F含量较高时易形成黑钨矿,F含量相对较低时容易形成白钨矿,而成矿流体的Ca^{2+}、Fe^{2+}、Mn^{2+}等含量及围岩岩性起次要或者局部作用。Wang et al.(2021)基于实验模拟研究提出了类似的观点,即在富F体系下,流体中的Ca^{2+}优先与F^-结合形成萤石,从而抑制了白钨矿的饱和沉淀,造成W主要以黑钨矿的形式产出。考虑到斑岩钨矿床通常缺乏富钙的围岩,F含量的高低很可能是控制斑岩钨矿床钨矿物种类的关键因素。

7 结 论

(1)类似于斑岩铜矿床,斑岩型钨矿亦主要分布于环太平洋成矿带与阿尔卑斯—喜马拉雅成矿带。斑岩钨矿床可形成于岩浆弧、板内及陆−陆碰撞等多种环境,且具有中生代大爆发的特点。

(2)斑岩型钨矿化与弱氧化、较高分异程度的I型或A型花岗岩类密切相关,不同于中国多数石英脉型、矽卡岩型钨矿与S型花岗岩类具有成因联系。与斑岩钨矿成矿有关的岩浆岩主要起源于古老地壳的重熔,并有少量亏损地幔和/或海洋沉积物的混染。

(3)斑岩钨矿成矿物质、成矿流体等主要来自于相关的岩浆岩。不同构造体制下斑岩钨矿床成矿流体系统具有一定差异:岩浆弧及板内环境下初始成矿流体多属于中高温、中高盐度的$NaCl-H_2O$系统;大陆碰撞体系下则多属于中高温、中低盐度的$NaCl-H_2O-CO_2$体系。

(4)斑岩钨矿床矿质沉淀机制主要包括流体不混溶/沸腾/CO_2逃逸±流体混合和水岩反应。岩浆−流体系统中F含量的高低很可能是控制斑岩钨矿床钨矿物种类的关键因素。

致谢:审稿专家和编辑老师对论文提出了宝贵的意见和建议,在此表示衷心的感谢!

References

Audétat A, Günther D, Heinrich C A. 2000. Magmatic−hydrothermal evolution in a fractionating granite: A microchemical study of the Sn−W−F−mineralized Mole granite (Australia)[J]. Geochimica et Cosmochimica Acta, 64(19): 3373−3393.

Ballouard C, Poujol M, Boulvais P, Branquet Y, Tartèse R, Vigneresse J L. 2016. Nb−Ta fractionation in peraluminous granites: A marker of the magmatic−hydrothermal transition[J]. Geology, 44(7): 231−234.

Bau M. 1996. Controls on the fractionation of isovalent trace elements in magmatic and aqueous systems: Evidence from Y/Ho, Zr/Hf, and lanthanide tetrad effect[J]. Contributions to Mineralogy and Petrology, 123(3): 323−333.

BGS. 2011. Tungsten[R]. British Geological Survey, Keyworth, UK. Available at: http://www.bgs.ac.uk/downloads/.

Blevin P L. 2004. Redox and compositional parameters for interpreting the granitoid metallogeny of eastern Australia: Implications for gold−rich ore systems[J]. Resource Geology, 54(3): 241−252.

Brand A A. 2008. Mineralogy, Geochemistry, and Geochronology of the Northern Dancer Tungsten- molybdenum Deposit, Yukon and British Columbia[D]. Vancouver: M.S. Thesis, University of British Columbia, 1-242.

Burnard P G, Polya D A. 2004. Importance of mantle derived fluids during granite associated hydrothermal circulation: He and Ar isotopes of ore minerals from Panasqueira[J]. Geochimica et Cosmochimica Acta, 68(7): 1607-1615.

Calvo G, Valero A, Valero A. 2019. How can strategic metals drive the economy? Tungsten and tin production in Spain during periods of war[J]. The Extractive Industries and Society, 6(1): 8-14.

Candela P A. 1992. Controls on ore metal ratios in granite-related ore systems: An experimental and computational approach[J]. Earth and Environmental Science Transactions of the Royal Society of Edinburgh, 83(1/2): 317-326.

Carpentier M, Chauvel C, Maury R C, Mattielli N. 2009. The "zircon effect" as recorded by the chemical and Hf isotopic compositions of Lesser Antilles forearc sediments[J]. Earth and Planetary Science Letters, 2009, 287(1/2): 86-99.

Chauvel C, Lewin E, Carpentier M, Arndt N T, Marini J C. 2008. Role of recycled oceanic basalt and sediment in generating the Hf-Nd mantle array[J]. Nature Geoscience, 1(1): 64-67.

Chelle-Michou C, Rottier B, Caricchi L, Simpson G. 2017. Tempo of magma degassing and the genesis of porphyry copper deposits[J]. Scientific Reports, 7: 40566.

Chen B, Ma X H, Wang Z Q. 2014. Origin of the fluorine-rich highly differentiated granites from the Qianlishan composite plutons (South China) and implications for polymetallic mineralization[J]. Journal of Asian Earth Sciences, 93: 301-314.

Chen Yanjing, Li Nuo. 2009. Nature of ore-fluids of intracontinental intrusion- related hypothermal deposits and its difference from those in island arcs[J]. Acta Petrologica Sinica, 25(10): 2477-2508 (in Chinese with English abstract).

Cooke D R, Hollings P, Walshe J L. 2005. Giant porphyry deposits: Characteristics, distribution, and tectonic controls[J]. Economic Geology, 100(5): 801-818.

Davis W J, Williams-Jones A E. 1985. A fluid inclusion study of the porphyry- greisen, tungsten- molybdenum deposit at Mount Pleasant, New Brunswick, Canada[J]. Mineralium Deposita, 20(2): 94-101.

Dewaele S, Clercq F D, Hulsbosch N, Piessens K, Boyce A, Burgess R, Muchez Ph. 2016. Genesis of the vein- type tungsten mineralization at Nyakabingo (Rwanda) in the Karagwe- Ankole belt, Central Africa[J]. Mineralium Deposita, 51(2): 283-307.

Du Yudiao, Yu Xinqi, Liu Jiajun, Zhou Xiang, Fu Jianzhen. 2012. Characteristics of ore- forming fluids and sources of ore- forming materials in the Dongyuan W- Mo deposit, Southern Anhui Province[J]. Geology in China, 38(5): 1334-1346(in Chinese with English abstract).

Feng Chengyou, Huang Fan, Zeng Zailin, Qu Wenjun, Ding Ming. 2011. Isotopic chronology of Jiulongnao granite and Hongshuizhai greisens- type tungsten deposit in South Jiangxi Province[J]. Journal of Jilin University (Earth Science Edition), 41(1): 111-121 (in Chinese with English abstract).

Fortier S M, Nassar N T, Lederer G W, Brainard J, Mccullough E A. 2018. Draft Critical Mineral List- Summary of Methodology and Background Information- US Geological Survey Technical Input Document in Response to Secretarial Order No. 3359[R]. US Geological Survey.

Gu Juyun. 1988. The characteristics of dominant porphyry tungsten deposits of China[J]. Mineral Resources and Geology, 2(1): 15-23 (in Chinese with English abstract).

Guo C L, Wang R C, Yuan S D, Wu S H, Yin B. 2015. Geochronological and geochemical constraints on the petrogenesis and geodynamic setting of the Qianlishan granitic pluton, Southeast China[J]. Mineralogy and Petrology, 109(2): 253-282.

Harris A C, Golding S D. 2002. New evidence of magmatic- fluid- related phyllic alteration: Implications for the genesis of porphyry Cu deposits[J]. Geology, 30(4): 335-338.

Hedenquist J W, Arribas A, Reynolds T J. 1998. Evolution of an intrusion- centered hydrothermal system: Far Southeast- Lepanto porphyry and epithermal Cu- Au deposits, Philippines[J]. Economic Geology, 93(4): 373-404.

Hou Zengqian, Yang Zhiming, Wang Rui, Zheng Yuanchuan. 2020. Further discussion on porphyry Cu-Mo-Au deposit formation in main- land China[J]. Earth Science Frontiers, 27(2): 20- 44(in Chinese with English abstract).

Huang H, Niu Y L, Mo X X. 2017. Garnet effect on Nd-Hf isotope decoupling: Evidence from the Jinfosi batholith, Northern Tibetan Plateau[J]. Lithos, 274: 31-38.

Hulsbosch N, Boiron M C, Dewaele S and Muchez P. 2016. Fluid fractionation of tungsten during granite- pegmatite differentiation and the metal source of peribatholitic W quartz veins: Evidence from the Karagwe- Ankole Belt (Rwanda) [J]. Geochimica et Cosmochimica Acta, 175(7): 299-318.

Inverno C M C, Hutchinson R W. 2006. Petrochemical discrimination of evolved granitic intrusions associated with Mount Pleasant deposits, New Brunswick, Canada[J]. Applied Earth Science, 115 (1): 23-39.

Jiang Shaoyong, Zhao Kuidong, Jiang Hai, Su Huimin, Xiong Suofei, Xiong Yiqu, Xu Yaoming, Zhang Wei, Zhu Lüyun. 2020. Spatiotemporal distribution, geological characteristics and metallogenic mechanism of tungsten and tin deposits in China: An overview[J]. Chinese Science Bulletin, 65(33): 86-101(in Chinese).

Keppler H, Wyllie P J. 1991. Partitioning of Cu, Sn, Mo, W, U, and Th between melt and aqueous fluid in the systems haplogranite-H_2O-HCl and haplogranite-H_2O-HF[J]. Contributions to Mineralogy and Petrology, 109(2): 139-150.

Kooiman G J A, McLeod M J, Sinclair W D. 1986. Porphyry tungsten-molybdenum orebodies, polymetallic veins and replacement bodies, and tin- bearing greisen zones in the Fire Tower Zone, Mount Pleasant, New Brunswick[J]. Economic Geology, 81(6): 1356−1373.

Kwark T A P, White A J R. 1982. Contrasting W−Mo−Cu and W−Sn−F skarn types and related granitoids[J]. Mining Geology, 32(174): 339−351.

Lecumberri- Sanchez P, Vieira R, Heinrich C A, Pinto F, Wälle M. 2017. Fluid- rock interaction is decisive for the formation of tungsten deposits[J]. Geology, 45(7): 579−582.

Lehmann B, Ishihara S, Michel H, Miller J, Winkelmann L. 1990. The Bolivian tin province and regional tin distribution in the Central Andes: A reassessment[J]. Economic Geology, 85(5): 1044−1058.

Li Hongying, Yang Lei, Chen Jianfeng. 2019. Geological characteristics and diagenetic age of ore−bearing rock of Taojiang Muguayuan tungsten deposit in Hunan Province[J]. Journal of Jilin University (Earth Science Edition), 49(5): 1285−1300(in Chinese with English abstract).

Li Jiadai, Li Xiaofeng. 2020. Research progress in metallogenesis of skarn−type tungsten deposits[J]. Mineral Deposit, 39(2): 256−272 (in Chinese with English abstract).

Li X Y, Gao J F, Zhang R Q, Lu J J, Chen W H, Wu J W. 2018. Origin of the Muguayuan veinlet- disseminated tungsten deposit, South China: Constraints from in−situ trace element analyses of scheelite[J]. Ore Geology Reviews, 99: 180−194.

Li Xianhai, Wang Dan, Wu Shangkun. 2014. The domestic strategic mineral resources evaluation index selection: Thinking based on list of key- minerals such as the United States, the European Union[J]. China Mining Magazine, 23(4): 30−33(in Chinese with English abstract).

Liu J, Li W C, Zhu X P, Li C, Zhou Q, Yang F C. 2020a. Origin and evolution of ore- forming fluids of the Larong W- (Mo) deposit, eastern Tibet: Constraints from fluid inclusions, H−O isotopes, and scheelite geochemistry[J]. Ore Geology Reviews, 124: 103620.

Liu J, Li W C, Zhu X P, Wang B D, Jiang J S, Liu H F. 2020b. Magmatic evolution and related W- Mo mineralization in the Larong deposit, eastern Tibet: Evidence from zircon U- Pb ages, geochemistry and Sr- Nd- Hf isotopes[J]. Ore Geology Reviews, 120: 103411.

Liu J, Li W C, Zhu X P, Zhou J X, Yu H J. 2020c. Ore genesis of the Late Cretaceous Larong porphyry W- Mo deposit, eastern Tibet: Evidence from in- situ trace elemental and S- Pb isotopic compositions[J]. Journal of Asian Earth Sciences, 190: 104199.

Liu Jun, Zhu Xiangping, Li Wenchang, Wang Baodi, Dong Yu, Yang Fucheng, Yang Houbin, Wu Jianghua. 2019. Molybdenite Re- Os dating of the Larong porphyry W−Mo deposit in eastern Tibet and its geological significance[J]. Acta Geologica Sinica, 93(7): 1708−1719(in Chinese with English abstract).

Liu P, Mao J W, Pirajno F, Jia L H, Zhang F, Li Y. 2018. Ore genesis and geodynamic setting of the Lianhuashan porphyry tungsten deposit, eastern Guangdong Province, SE China: Constraints from muscovite ^{40}Ar- ^{39}Ar and zircon U- Pb dating and Hf isotopes[J]. Mineralium Deposita, 53(6): 797−814.

Lowell J D, Guilbert J M. 1970. Lateral and vertical alteration−mineralization zoning in porphyry ore deposits[J]. Economic Geology, 65(4): 373−408.

Lu H Z, Liu Y M, Wang C L, Xu Y Z, Li H Q. 2003. Mineralization and fluid inclusion study of the Shizhuyuan W- Sn- Bi- Mo- F skarn deposit, Hunan Province, China[J]. Economic Geology, 98 (5): 955−974.

Lu H Z. 1985. Fluid inclusion studies of a new type of ore deposit: Porphyry tungsten occurrence in China[J]. Geochemistry, 4(1): 41−53.

Mao J W, Cheng Y B, Chen M H, Franco P. 2013. Major types and time- space distribution of Mesozoic ore deposits in South China and their geodynamic settings[J]. Mineralium Deposita, 48(3): 267−294.

Mao J W, Xiong B K, Liu J, Franco P, Cheng Y B, Ye H S, Song S W, Dai P. 2017a. Molybdenite Re/Os dating, zircon U- Pb age and geochemistry of granitoids in the Yangchuling porphyry W- Mo deposit (Jiangnan tungsten ore belt), China: Implications for petrogenesis, mineralization and geodynamic setting[J]. Lithos, 286/287: 35−52.

Mao Jingwen, Wu Shenghua, Song Shiwei, Dai Pan, Xie Guiqing, Su Qiangwei, Liu Peng, Wang Xianguang, Yu Zhongzhen, Chen Xiangyun, Tang Weixin. 2020. The world−class Jiangnan tungsten belt: Geological characteristics, metallogeny, and ore deposit model [J]. Chinese Science Bulletin, 65(33): 102−118(in Chinese).

Mao W, Rusk B, Yang F C, Zhang M J. 2017b. Physical and chemical evolution of the Dabaoshan porphyry Mo deposit, south China: Insights from fluid inclusions, cathodoluminescence, and trace elements in quartz[J]. Economic Geology, 112(4): 889−918.

Meinert L D, Hedenquist J W, Satoh H, Matsuhisa, Y. 2003. Formation of anhydrous and hydrous skarn in Cu- Au ore deposits by magmatic fluids[J]. Economic Geology, 98(1): 147−156.

Mo Mingzhen. 1988. A preliminary study on alteration zoning of the Yangchuling porphyry W- Mo deposit and its relationship to mineralization[J]. Mineral Deposit, 7(3): 52- 61(in Chinese with English abstract).

Mortensen J K, Brand A, Liverton T. 2006. Laser ablation ICP−MS U−Pb zircon ages for Cretaceous plutonic rocks in the Logtung and Thirtymile Range areas of southern Yukon[C]//Emond D S, Lewis L L, Weston L H (eds.). Yukon Exploration and Geology. Yukon Geological Survey.

Mustard R, Ulrich T, Kamenetsky V S, Mernagh T. 2006. Gold and metal enrichment in natural granitic melts during fractional crystallization[J]. Geology, 34(2): 85−88.

Nast H J, Williams- Jones A E. 1991. The role of water- rock interaction and fluid evolution in forming the porphyry- related

Sisson Brook W-Cu-Mo deposit, New Brunswick[J]. Economic Geology, 86(2): 302-317.

Ni P, Wang X D, Wang G G, Huang J B, Wang T G. 2015. An infrared microthermometric study of fluid inclusions in coexisting quartz and wolframite from Late Mesozoic tungsten deposits in the Gannan metallogenic belt, South China[J]. Ore Geology Reviews, 65: 1062-1077

Nie Rongfeng, Wang Xudong. 2007. On research advancement of Southern Jiangxi's tungsten deposits[J]. China Mining Magazine, 22 (3): 4-8(in Chinese with English abstract).

Noble S R, Spooner E T C, Harris F R. 1984. The Logtung large tonnage, low-grade W (scheelite)-Mo porphyry deposit, south-central Yukon Territory[J]. Economic Geology, 79(5): 848-868.

Pan X F, Hou Z Q, Zhao M, Chen G H, Rao J F, Li Y, Wei J, Ouyang Y P. 2018. Geochronology and geochemistry of the granites from the Zhuxi W-Cu ore deposit in South China: Implication for petrogenesis, geodynamical setting and mineralization[J]. Lithos, 304: 155-179.

Patchett P J, White W M, Feldmann H, Kielinczuk S, Hofmann A W. 1984. Hafnium/rare earth element fractionation in the sedimentary system and crustal recycling into the Earth's mantle[J]. Earth and Planetary Science Letters, 69(2): 365-378.

Qin Yan, Wang Denghong, Wu Libin, Wang Keyou, Mei Yuping. 2010. Zircon SHRIMP U-Pb dating of the mineralized porphyry in the Dongyuan W deposit in Anhui Province and its geological significance[J]. Acta Geologica Sinica, 84(4): 479-484(in Chinese with English abstract).

Rudnick R L, Gao S. 2003. Composition of the continental crust[J]. Treatise Geochem., 3: 659.

Sanfilippo A, Salters V, Tribuzio R, Zanetti A. 2019. Role of ancient, ultra-depleted mantle in Mid-Ocean-Ridge magmatism[J]. Earth and Planetary Science Letters, 511: 89-98.

Schmitz M D, Vervoort J D, Bowring S A, Patchett P J. 2004. Decoupling of the Lu-Hf and Sm-Nd isotope systems during the evolution of granulitic lower crust beneath southern Africa[J]. Geology, 32(5): 405-408.

Seal R R. 2006. Sulfur isotope geochemistry of sulfide minerals[J]. Reviews in Mineralogy and Geochemistry, 61(1): 633-677.

Selby D, Creaser R A, Heaman L M, Hart C J. 2003. Re-Os and U-Pb geochronology of the Clear Creek, Dublin Gulch, and Mactung deposits, Tombstone Gold Belt, Yukon, Canada: Absolute timing relationships between plutonism and mineralization[J]. Canadian Journal of Earth Sciences, 40(12): 1839-1852.

Shan Liang, Pang Yingchun, Ke Xianzhong, Liu Jiajun, Chen Wenhui, Niu Zhijun, Xu Deming, Long Wenguo, Wang Binqing. 2019. Diagenetic and metallogenic age of the Muguayuan tungsten polymetallic deposit and its effect on regional mineralization, Taojiang County, Northeastern Hunan Province, China[J]. Geological Science and Technology Information, 38(1): 100-112 (in Chinese with English abstract).

Sheng J F, Liu L J, Wang D H, Chen Z H, Ying L J, Huang F, Wang J H, Zeng L. 2015. A preliminary review of metallogenic regularity of tungsten deposits in China[J]. Acta Geologica Sinica(English Edition), 89(4): 1359-1374.

Shi Hongzhao, Lin Fangcheng, Zhang Linkui. 2009. Spatio-temporaldistribution and current state ofthe research of the tungsten deposits: An overview[J]. Sedimentary Geology and Tethyan Geology, 29(4): 90-95(in Chinese with English abstract).

Shimazaki H. 1980. Characteristics of skarn deposits and related acid magmatism in Japan[J]. Economic Geology, 75(2): 173-183.

Sillitoe R H. 2010. Porphyry copper systems[J]. Economic Geology, 105(1): 3-41.

Sinclair W D.1995. Porphyry W. Selected British Columbia Mineral Deposit Profiles, Volume 1-metallics and coal[C]//Lefebure D V , Ray G E(eds.). British Columbia Ministry of Energy of Employment and Investment, Open File 1995-20: 101-104.

Sun S S, McDonough W F. 1989. Chemical and isotopic systematics of oceanic basalts: Implications for mantle composition and processes[J]. Geological Society, London, Special Publications, 42 (1): 313-345.

Tan Yunjin. 1985. Metallogenetic mechanism of Lianhuashan porphyry tungsten deposit[J]. Science in China (Series B), (6): 83-90(in Chinese).

Tan Yunjin. 1999. Composite characteristic of tungsten minerals and its dominate factors of endogenesis tungsten deposit in south China[J]. China Tungsten Industry, 14(5/6): 84-89(in Chinese).

Tang M, Wang X L, Shu X J, Wang D, Yang T, Gopon P. 2014. Hafnium isotopic heterogeneity in zircons from granitic rocks: Geochemical evaluation and modeling of "zircon effect" in crustal anatexis[J]. Earth and Planetary Science Letters, 389: 188-199.

Taylor H P. 1974. The application of oxygen and hydrogen isotope studies to problems of hydrothermal alteration and ore deposition[J]. Economic Geology, 69(6): 843-883.

Thode H G, Monster J, Dunford H B. 1961. Sulphur isotope geochemistry[J]. Geochimica et Cosmochimica Acta, 25(3): 159-174.

Thorne K G, Fyffe L R, Creaser R A. 2013. Re-Os geochronological constraints on the W-Mo mineralizing event in the Mount Pleasant Caldera Complex: Implications for the timing of subvolcanic magmatism and caldera development[J]. Atlantic Geology, 49(1): 131-150.

Ulrich T, Mavrogenes J. 2008. An experimental study of the solubility of molybdenum in H_2O and KCl-H_2O solutions from 500℃ to 800℃, and 150 to 300 MPa[J]. Geochimica et Cosmochimica Acta, 72(9): 2316-2330.

Vallance J, Cathelineau M, Marignac C, Boiron M C, Cécile F. 2001. Microfracturing and fluid mixing in granites: W- (Sn) ore deposition at Vaulry (NW French Massif Central) [J]. Tectonophysics, 336(1/4): 43-61.

Vervoort J D, Blichert-Toft J. 1999. Evolution of the depleted mantle: Hf isotope evidence from juvenile rocks through time[J].

Geochimica et Cosmochimica Acta, 63(3/4): 533−556.

Vervoort J D, Plank T, Prytulak J. 2011. The Hf−Nd isotopic composition of marine sediments[J]. Geochimica et Cosmochimica Acta, 75(20): 5903−5926.

Voicu G, Bardoux M, Stevenson R, Jebrak M. 2000. Nd and Sr isotope study of hydrothermal scheelite and host rocks at Omai, Guiana Shield: Implications for ore fluid source and flow path during the formation of orogenic gold deposits[J]. Mineralium Deposita, 35 (4): 302−314.

Wade J, Wood B J, Norris C A. 2013. The oxidation state of tungsten in silicate melt at high pressures and temperatures[J]. Chemical Geology, 335: 189−193.

Wang Denghong, Xu Zhigang, Sheng Jifu, Zhu Mingyu, Xu Jue, Yuan Zhongxin, Bai Ge, Qu Wenjun, Li Huaqin, Chen Zhenghui, Wang Chenghui, Huang Fan, Zhang Changqing, Wang Yonglei, Ying Lijuan, Li Houmin, Gao Lan, Sun Tao, Fu Yong, Li Kangjian, Wu Guang, Tang Juxing, Feng Chengyou, Zhao Zheng, Zhang Daquan. 2014. Progress on the study of regularity of major mineral resources and regional metallogenic regularity in China: A Review[J]. Acta Geologica Sinica, 88(12): 2176−2191(in Chinese with English abstract).

Wang Lijuan, Wang Jingbin, Wang Yuwang, Wang Junsheng, Liao Zhen. 2011. The characteristics of porphyry Cu, Mo, W ore−forming fluid in different tectonic setting[J]. Mineral Exploration, 2 (6): 704−713(in Chinese with English abstract).

Wang P, Chen Y J, Fu B, Yang Y F, Mi M, Li Z L. 2014. Fluid inclusion and H−O−C isotope geochemistry of the Yaochong porphyry Mo deposit in Dabie Shan, China: A case study of porphyry systems in continental collision orogens[J]. International Journal of Earth Sciences, 103(3): 777−797.

Wang X L, Qiu Y, Chou I M, Zhang R Q, Li G L, Zhong R C. 2020. Effects of pH and salinity on the hydrothermal transport of tungsten: Insights from in situ Raman spectroscopic characterization of K_2WO_4−NaCl−HCl−CO_2 solutions at temperatures up to 400℃[J]. Geofluids, 2: 1−12.

Wang X S, Williams−Jones A E, Hu R Z, Shang L B, Bi X W. 2021. The role of fluorine in granite−related hydrothermal tungsten ore genesis: Results of experiments and modeling[J]. Geochimica et Cosmochimica Acta, 292: 170−187.

Wang Xue, Huang Xiaolong, Ma Jinlong, Zhong Junwei, Yang Qijun. 2015. Hf−Nd isotopes of the Early Precambrian metamorphic complexes in the southern segment of the Trans−North China Orogen: Implications for crustal evolution[J]. Geotectonica et Metallogenia, 39(6): 1108−1118(in Chinese with English abstract).

Wang Y H, Zhang F F, Liu J J, Xue C Ji, Zhang Z C. 2018. Genesis of the Wurinitu W−Mo deposit, Inner Mongolia, northeast China: Constraints from geology, fluid inclusions and isotope systematics[J]. Ore Geology Reviews, 94: 367−382.

Wood S A, Samson I M. 2000. The hydrothermal geochemistry of tungsten in granitoid environments: I. Relative solubilities of ferberite and scheelite as a function of T, P, pH, and mNaCl[J]. Economic Geology, 95(1): 143−182.

Wu F Y, Liu X C, Ji W Q, Wang J M, Yang L. 2017. Highly fractionated granites:Recognition and research[J]. Science China Earth Sciences, 60(7): 1201−1219.

Xu Keqin, Liu Yingjun, Yu Shoujun. 1959. Types of tungsten deposits of China and their distribution with relation to geotectonics [J]. Journal of Nanjing University (Natural Sciences), (2): 31−54(in Chinese with English abstract).

Xu Tai, Gao Haidong, Li Yuanzhi, Wei Xin. 2012. On the metallogenic characteristics of China's tungsten deposits[J]. China Tungsten Industry, 27(3): 1−5(in Chinese with English abstract).

Yuan Shunda, Zhang Dongliang, Shuang Yan, Du Andao, Qu Wenjun. 2012. Re−Os dating of molybdenite from the Xintianling giant tungsten−molybdenum deposit in southern Hunan Province, China and its geological implications[J]. Acta Petrologica Sinica, 28(1): 27−38(in Chinese with English abstract).

Zartman R E, Doe B R. 1981. Plumbotectonics− the model[J]. Tectonophysics, 75(1/2): 135−162.

Zhai Yusheng. 2002. Some features of regional metallogeny of China[J]. Geology and Exploration, 38(5):1−4(in Chinese with English abstract).

Zhang C, Santosh M, Luo Q, Jiang S, Liu L F, Liu D D. 2019. Impact of residual zircon on Nd−Hf isotope decoupling during sediment recycling in subduction zone[J]. Geoscience Frontiers, 10(1): 241−251.

Zhang Dachun, Mu Zhiguo, Huang Fusheng, Chen Chengye, Zheng Shuhui. 1984. Stable isotope studied of the Yangchuling tungsten−molybdenum ore deposit, Jiangxi Province[J]. Mineral Deposits, 3 (02): 56−65(in Chinese with English abstract).

Zhang Jiajing, Chen Zhenghui, Wang Denghong, Chen Zhenyu, Liu Shanbao, Wang Chenghui. 2008. Geological characteristics and metallogenic epoch of the Xingluokeng tungsten deposit, Fujian Province[J]. Geotectonica et Metallogenia, 32(1): 92−97(in Chinese with English abstract).

Zhang Ligang. 1985. Hydrogen, oxygen, sulfur and carbon isotope geochemistry of the Lianhuashan porphyry type tungsten deposit[J]. Mineral Deposits, 4(1): 56−65(in Chinese with English abstract).

Zhang W, Lentz D R, Thorne K G, Massawe R J R. 2020. Late Silurian−Early Devonian slab break−off beneath the Canadian Appalachians: Insights from the Nashwaak granite, west−central New Brunswick, Canada[J]. Lithos, 358/359: 105393.

Zhang W, Lentz D R, Thorne K G, McFarlane C. 2016. Geochemical characteristics of biotite from felsic intrusive rocks around the Sisson Brook W−Mo−Cu deposit, west−central New Brunswick: An indicator of halogen and oxygen fugacity of magmatic systems[J]. Ore Geology Reviews, 77: 82−96.

Zhang Yuxue. 1982. Geological characteristics and origin of Yangchuling porphyry W−Mo deposit[J]. Geochimica, (2): 122−132(in Chinese with English abstract).

Zhao W W, Zhou M F, Li Y H M, Zhao Z, Gao J F. 2017. Genetic types, mineralization styles, and geodynamic settings of Mesozoic tungsten deposits in South China[J]. Journal of Asian Earth Sciences, 137: 109−140.

Zhou Jie. 2013. Origin of Tungsten−bearing Granites in the Eastern Jiangnan Orogen Belt[D]. Nanjing: Nanjing University, 1−95(in Chinese with English abstract).

Zhou Xiang, Yu Xinqi, Wang De'en, Zhang Dehui, Li Chunlin, Fu Jianzhen, Dong Hhuiming. 2011. Characteristics and geochronology of the W, Mo−bearing granodiorite porphyry in Dongyuan, Southern Anhui[J]. Geoscience, 25(2): 201−210(in Chinese with English abstract).

Zhu Bingquan. 1998. Theories and Application of Isotopic System in Geoscience: Crustal and Mantle Evolution in China continent[M]. Beijing: Science Press, 224−226(in Chinese).

Zhu Xinyou, Wang Jingbin, Wang Yanli, Cheng Xiyin, He Peng, Fu Qibin, Li Tingshun. 2013. Characteristics of greisen inclusions in alkali feldspar granite of Yaogangxian tungsten deposit[J]. Mineral Deposits, 32(3): 533−544(in Chinese with English abstract).

附中文参考文献

陈衍景, 李诺. 2009. 大陆内部浆控高温热液矿床成矿流体性质及其与岛弧区同类矿床的差异[J]. 岩石学报, 25(10): 2477−2508.

杜玉雕, 余心起, 刘家军, 周翔, 傅建真. 2012. 皖南东源钨钼矿成矿流体特征和成矿物质来源[J]. 中国地质, 38(5): 1334−1346.

丰成友, 黄凡, 曾载淋, 屈文俊, 丁明. 2011. 赣南九龙脑岩体及洪水寨云英岩型钨矿年代学[J]. 吉林大学学报(地球科学版), 41(1): 111−121.

古菊云. 1988. 中国主要斑岩钨矿床特征[J]. 矿产与地质, 2(1): 15−23.

侯增谦, 杨志明, 王瑞, 郑远川. 2020. 再论中国大陆斑岩Cu−Mo−Au矿床成矿作用[J]. 地学前缘, 27(2): 20−44.

蒋少涌, 赵葵东, 姜海, 苏慧敏, 熊索菲, 熊伊曲, 徐耀明, 章伟, 朱律运. 2020. 中国钨锡矿床时空分布规律、地质特征与成矿机制研究进展[J]. 科学通报, 65(33): 86−101.

李洪英, 杨磊, 陈剑锋. 2019. 湖南桃江县木瓜园钨矿床地质特征及含矿岩体成岩时代[J]. 吉林大学学报(地球科学版), 49(5): 1285−1300.

李佳黛, 李晓峰. 2020. 矽卡岩型钨矿床成矿作用研究进展[J]. 矿床地质, 39(2): 256−272.

李宪海, 王丹, 吴尚昆. 2014. 我国战略性矿产资源评价指标选择: 基于美国、欧盟等关键矿产名录的思考[J]. 中国矿业, 23(4): 30−33.

刘俊, 祝向平, 李文昌, 王保弟, 董宇, 杨富成, 杨后斌, 吴江华. 2019. 藏东拉荣斑岩钨钼矿床辉钼矿Re−Os定年及地质意义[J]. 地质学报, 93(7): 1708−1719.

毛景文, 吴胜华, 宋世伟, 戴盼, 谢桂青, 苏蔷薇, 刘鹏, 王先广, 余忠珍, 陈祥云, 唐维新. 2020. 江南世界级钨矿带:地质特征、成矿规律和矿床模型[J]. 科学通报, 65(33): 102−118.

莫名浈. 1988. 阳储岭斑岩钨钼矿床蚀变分带特征及与成矿作用关系的初步研究[J]. 矿床地质, 7(3): 52−61.

聂荣锋, 王旭东. 2007. 赣南钨矿研究进展[J]. 中国钨业, 22(3): 4−8.

秦燕, 王登红, 吴礼彬, 王克友, 梅玉萍. 2010. 安徽东源钨矿含矿斑岩中的锆石SHRIMP U−Pb年龄及其地质意义[J]. 地质学报, 84(4): 479−484.

陕亮, 庞迎春, 柯贤忠, 刘家军, 陈文辉, 牛志军, 徐德明, 龙文国, 王滨清. 2019. 湖南省东北部地区桃江县木瓜园钨多金属矿成岩成矿时代及其对区域成矿作用的启示[J]. 地质科技情报, 38(1): 100−112.

石洪召, 林方成, 张林奎. 2009. 钨矿床的时空分布及研究现状[J]. 沉积与特提斯地质, 29(4): 90−95.

谭运金. 1985. 莲花山斑岩钨矿床的成矿机理[J]. 中国科学(B辑), (6): 83−90.

谭运金. 1999. 华南地区内生钨矿床的钨矿物成分特征及其控制因素[J]. 中国钨业, 14(5−6): 84−89.

王登红, 徐志刚, 盛继福, 朱明玉, 徐珏, 袁忠信, 白鸽, 屈文俊, 李华芹, 陈郑辉, 王成辉, 黄凡, 张长青, 王永磊, 应立娟, 李厚民, 高兰, 孙涛, 付勇, 李建康, 武广, 唐菊兴, 丰成友, 赵正, 张大权. 2014. 全国重要矿产和区域成矿规律研究进展综述[J]. 地质学报, 88(12): 2176−2191.

王莉娟, 王京彬, 王玉往, 王军升, 廖震. 2011. 不同构造环境中的斑岩铜,钼,钨等矿床成矿流体特征[J]. 矿产勘查, 2(6): 704−713.

王雪, 黄小龙, 马金龙, 钟军伟, 杨启军. 2015. 华北克拉通中部造山带南段早前寒武纪变质杂岩的Hf−Nd同位素特征及其地壳演化意义[J]. 大地构造与成矿学, 39(6): 1108−1118.

徐克勤, 刘英俊, 俞受鋆. 1959. 中国钨矿的类型及其分布规律[J]. 南京大学学报(自然科学版), (2): 31−54.

许泰, 高海东, 李元志, 魏欣. 2012. 中国钨矿床成矿特征探讨[J]. 中国钨业, 27(3): 1−5.

袁顺达, 张东亮, 双燕, 杜安道, 屈文俊. 2012. 湘南新田岭大型钨钼矿床辉钼矿Re−Os同位素测年及其地质意义[J]. 岩石学报, 28(1): 27−38.

翟裕生. 2002. 中国区域成矿特征探讨[J]. 地质与勘探, 38(5): 1−4.

张大椿, 穆治国, 黄福生, 陈成业, 郑淑蕙. 1984. 江西阳储岭钨钼矿床稳定同位素组成特征的研究[J]. 矿床地质, 3(2): 56−65.

张家菁, 陈郑辉, 王登红, 陈振宇, 刘善宝, 王成辉. 2008. 福建行洛坑大型钨矿的地质特征, 成矿时代及其找矿意义[J]. 大地构造与成矿学, 32(1): 92−97.

张理刚. 1985. 莲花山斑岩型钨矿床的氢、氧、硫、碳和铅同位素地球化学[J]. 矿床地质, 4(1): 56−65.

张玉学. 1982. 阳储岭斑岩钨钼矿床地质地球化学特征及其成因探讨[J]. 地球化学, (2): 122−132.

周洁. 2013. 江南造山带东段含钨花岗岩成因研究[D]. 博士学位论文. 南京: 南京大学, 1−95.

周翔, 余心起, 王德恩, 张德会, 李春麟, 傅建真, 董会明. 2011. 皖南东源含W、Mo花岗闪长斑岩及成岩成矿年代学研究[J]. 现代地质, 25 (2): 201−210.

朱炳泉. 1998. 地球科学中同位素体系理论与应用——兼论中国大陆壳幔演化[M]. 北京: 科学出版社, 224−226.

祝新友, 王京彬, 王艳丽, 程细音, 何鹏, 傅其斌, 李顺庭. 2013. 黑钨矿矿床中云英岩包体及岩浆液态分异成矿研究——以湖南瑶岗仙钨矿为例[J]. 矿床地质, 32(3): 533−544.